Identification of Copper(II) Binding Sites in the Aminoglycosidic Antibiotic Neomycin B

Małgorzata Jeżowska-Bojczuk,*[a] Wojciech Szczepanik,[a][‡] Stefano Mangani,[b] Elena Gaggelli,[b] Nicola Gaggelli,[b] and Gianni Valensin[b]

Keywords: Bioinorganic chemistry / Aminoglycoside antibiotics / Neomycin B / N,O ligands / Copper

Protonation and copper(II) coordination properties of neomycin B were studied in solution by potentiometry, NMR, UV/Vis, CD, and EPR spectroscopy, XAS and mass spectrometry. Mono- and dinuclear complexes were found depending on the metal-to-ligand molar ratio. Neomycin B anchors Cu^{II} ions above pH 5.0 with an NH_2 group from ring B. Simultaneously, the second amino group of the same ring and the hydroxyl group of ring A complete the binding set of donors. With an increase in pH the remaining $-NH_3^+$ functional groups in the neomycin B molecule are deprotonated without affecting the complexation pattern. However, these groups, particularly the ones located in the D-ring of the antibiotic, may coordinate the second copper(II) ion when the metal is present in excess. We have proved this process with the use of potentiometry, CD and especially mass spectrometry.

Introduction

Neomycins are aminoglycoside antibiotics produced by *Streptomyces fradiae* as a mixture of three analogues A, B and C. Only neomycin B is used in therapy and it is active against gram-negative aerobic bacteria and *Staphylococcus.* It is topically or orally applied, mainly prior to surgical interventions of the intestine. Parenteral administration of the drug may result in oto- and nephrotoxic effects much more acute than for any other aminoglycoside.[1] A possible explanation was recently provided in our studies,[2] showing that (i) neomycin has the highest potency in cleaving $tRNA^{Phe}$ and (ii) the Cu^{II}-neomycin complex disproportionates H_2O_2 to hydroxyl radicals, as well as oxidizes plasmid DNA with the highest efficiency.

Coordination of aminoglycosides by Cu^{II} ions was extensively investigated[3–6] and evidence was reached for copper selectively yielding high stability complexes over other transition metal ions.[7] Although not present at very high levels intracellularly, the amount of copper(II) in the plasma reflects the state of health of the organism. Under circumstances when antibiotics are applied (e.g. inflammation), the serum level of copper may drastically increase,[8] probably as a result of leukocyte activation that releases even micromolar amounts of copper and iron as well.[9] Increased concentrations of Cu^{II} ions in selected tissues are also observed during the appearance of cancer, anemia[10] or hyperthyroidism.[11] Thus chelation of the metal by xenobiotics, e.g. drugs, may occur in vivo.

The coordination abilities of neomycin B (Figure 1) have not been thoroughly investigated to date. Formation of solid polymeric complexes has been observed with selected transition metal ions but without any evidence of amino groups being involved in binding.[12] The characteristics of the Cu^{II} complex of neomycin B in solution have also been delineated, but the final determined structure concerns only the coordination of neamine,[13] a subunit of neomycin B

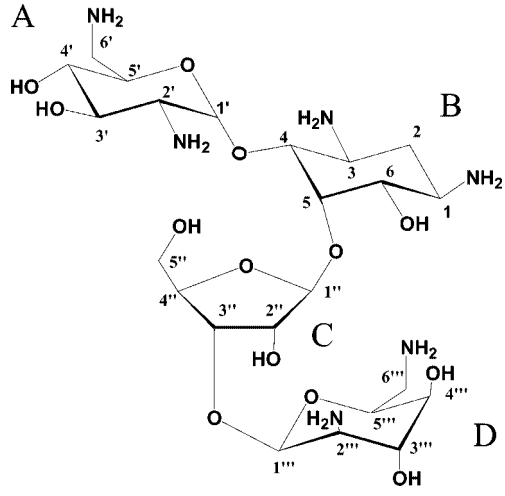

Figure 1. Molecular structure of neomycin B.

[a] Faculty of Chemistry, University of Wrocław,
F. Joliot-Curie 14, 50-383 Wrocław, Poland
Fax: +48-71-3282-348
E-mail: mjb@wchuwr.chem.uni.wroc.pl
[b] Department of Chemistry, University of Siena,
Via Aldo Moro, 53100 Siena, Italy
[‡] Supported by the Foundation for Polish Science (FNP) with the Annual Stipend for Young Scientists.
Supporting information for this article is available on the WWW under http://www.eurjic.org or from the author.

(see rings A and B, Figure 1). The aim of the current study is to gain deeper insight into the Cu^{II}-neomycin binding equilibria depending upon pH and metal ion-to-antibiotic molar ratio.

Results and Discussion

Protonation of Neomycin B

The protonation constants calculated on the basis of potentiometric titrations are presented in Table 1. They correspond to six amino groups present in this hexaprotic antibiotic molecule. Both amino sugar rings (A and D) and the 2-deoxystreptamine ring (B) contain two amino group substituents. Only the pentose ring (C) has no protonating function (Figure 1). The location of the amino groups causes equal distribution of the positive charge within the neomycin B molecule.

Table 1. Protonation and stability constants of neomycin B and its copper(II) complexes.

Protonation constants of neomycin B			Stability constants of Cu^{II}-neomycin B		
species	log β	pK	species	log β	pK
LH_6	46.575(2)	5.69	CuH_3L	31.80(4)	–
LH_5	40.885(2)	7.02	CuH_2L	26.24(1)	5.56
LH_4	33.865(2)	7.603	CuHL	19.02(1)	7.22
LH_3	26.262(3)	8.147	CuL	10.94(1)	8.08
LH_2	18.115(2)	8.745	$CuH_{-1}L$	1.97(1)	8.97
LH	9.370(2)	9.370	$CuH_{-2}L$	–7.99(1)	9.96

Almost all pK_a values are typical for amino functions and fit the characteristic range 7–9 (Table 1), except the first one which is much lower (pK_a = 5.69) in agreement with previous ^{15}N NMR spectroscopic measurements.[14] Such low values of the first deprotonation constant were also found for all other aminoglycosides studied so far: 6.0 for geneticin[3] and kanamycin A[4] that have a +4 charge at low pH, and 5.7 for the +5 charged kanamycin B[5] and tobramycin.[6] Neomycin with its six amines has an almost identical value for this constant as do the pentaprotic antibiotics. Therefore, the decrease in the first pK_a of the aminoglycosides is likely to arise from a local electrostatic interaction between neighboring NH_3^+ groups within the same ring,[4,5,14] rather than from the overall charge of the entire molecule.

All the successive deprotonations are separated from one another by only ca. 0.6 log units (Table 1). The statistics on the deprotonation of bifunctional molecules indicate that each of the two processes is almost parallel (the "ideal" statistical log value is 0.6[15]). ^{15}N NMR spectroscopy allowed us to calculate the pK values and assign them to each amino group of the antibiotic molecule.[14] In spite of diverse experimental conditions, the calculated constants agree with our determinations.

Copper(II) Complexation by Neomycin B

Neomycin B offers more potential possibilities for copper(II) chelation when compared with previously investigated aminoglycoside antibiotics.[3–6] This antibiotic forms six complexes with cupric ion in the pH range 5.5 to 10. At a 1:1 molar ratio or at an excess of the antibiotic, only monomeric complexes are formed in solution, as confirmed by potentiometry and mass spectrometry measurements (Table 1 and Table 2). The first minor species, which starts to occur at pH ca. 5, has CuH_3L stoichiometry (H_6L represents the fully protonated ligand). It is a common feature of the Cu^{II}-aminoglycoside complexes that the binding process is accompanied by a two-proton loss, which results from chelate ring formation by the amine nitrogen and a neighboring hydroxyl oxygen with simultaneous deprotonation of the latter. Cu^{II} anchoring then proceeds at the 3 amino group of the deoxystreptamine ring B due to its lowest deprotonation constant value.[14] In the case of neomycin B there is an additional deprotonation of another amine function. This event is very likely to occur at one of the bisaminated rings (A or D) due to the mentioned electrostatic interaction, but not in ring (B), where Cu^{II} is already bound. A {N,O} type chelation therefore occurs, with deprotonation of another amine, without its involvement in coordination. However, the CuH_3L species exists at too low

Table 2. Summary of the observed ESI-MS ions (m/z) at pH 8.0 {$(NH_4)_2CO_3$, 5 mM} for neomycin B (L) and its Cu^{II} complex. Concentrations: Cu^{II} 0.25 or 0.5 mM and L 0.25 mM.

Components	$m/z_{obsd.}$	$m/z_{calcd.}$	Assignment
neomycin B	308.5[w]	308.4	L – rings C and D + H^+
	456.3[w]	455.5	L – ring A or D + H^+
	616.5[s]	615.6	L + H^+
Cu^{II}-neomycin, 1:1	371.4[s]	370.9	Cu^{II}–L – rings C and D – OH + H^+
	388.3[i]	387.9	Cu^{II}–L – rings C and D + H + H^+
	503.4[w]	503.0	Cu^{II}–L – ring A or D – OH + H^+
	677.7[i]	677.3	Cu^{II}–L + H^+
			and all peaks seen for neomycin B
Cu^{II}-neomycin, 2:1	446.4[w]	446.1	Cu^{II}_2–L – rings C and D + H + H^+
	738.9[i]	738.2	Cu^{II}_2–L + H+
			and all peaks seen for neomycin B
			and Cu^{II}-neomycin B, 1:1

w – weak, i – intermediate, s – strong signal.

a fraction (12% of total Cu^{II} amount, Figure 2) to allow unambiguous delineation of its characteristics.

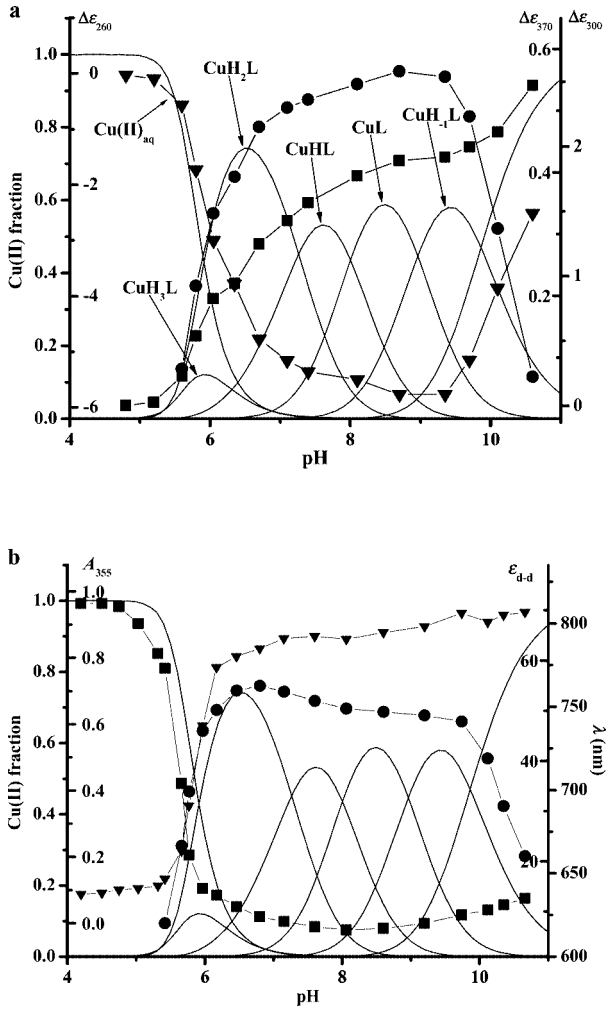

Figure 2. The speciation diagram for the Cu^{II}-neomycin B system with CD spectral parameters overlaid (a): $\Delta\varepsilon$ of CT bands at: 260 nm (▼), 300 nm (■) and 370 nm (●), as well as UV/Vis spectra parameters overlaid (b): ε (▼) and λ (■) of d-d band and shoulder at 355 nm (●). $\Delta\varepsilon$ and ε are in M^{-1} cm^{-1}.

This form is followed by a major species, CuH_2L complex, which prevails over the first at almost the same pH range. The stability constants of both complexes differ by ca. 5.6 log units, in agreement with the deprotonation of another amine nitrogen. However, this value is too low for a spontaneous proton loss and seems to be forced by another electron pair acceptor. If this further deprotonation proceeds at the same ring, where Cu^{II} is already bound, then another deprotonated nitrogen will also be engaged in the coordination process and {N,N,O} type chelation will occur. The results, obtained from spectroscopic measurements confirm that the CuH_2L species involves two nitrogen atoms coordinated to the central metal ion.

In order to establish the coordination pattern of this species unambiguously, ^1H and ^{13}C NMR spectroscopic methods were applied. The chemical shifts (ppm) of neomycin B are summarized in Table 3. Spectral assignment was achieved by COSY and ROESY experiments, by ^{13}C ^1H 2D shift correlated maps and by comparison with reference data.[16,17] Addition of copper to the solution of neomycin and pH adjustment to 6.8, where the CuH_2L complex reaches its maximum concentration, were not very effective in enhancing the nuclear relaxation rates. This fact is reflected by the relatively small values of R_{1p} (Table 4), where R_{1p}, the paramagnetic contribution to the spin-lattice relaxation is defined by Equation (1).

Table 3. ^1H and ^{13}C NMR chemical shift (ppm) of neomycin B 9.9 mM in D_2O at pH 6.8 (value uncorrected for the isotopic effect), T = 298 K and with TSP-d_4 as internal reference standard.

Ring	Proton	δ (ppm)	Carbon	δ (ppm)
B	1	3.31	1	54.04
	2_{ax}, 2_{eq}	1.73, 2.33	2	34.32
	3	3.28	3	51.87
	4	3.70	4	81.92
	5	3.90	5	88.24
	6	3.70	6	76.30
A	1′	5.97	1′	98.72
	2′	3.43	2′	56.98
	3′	3.99	3′	72.24
	4′	3.25	4′	73.95
	5′	4.06	5′	71.87
	$6'_{a,b}$	3.49, 3.28	6′	43.27
C	1′′	5.42	1′′	113.00
	2′′	4.45	2′′	76.39
	3′′	4.57	3′′	78.07
	4′′	4.24	4′′	84.09
	$5''_{a,b}$	3.93, 3.77	5′′	63.40
D	1′′′	5.31	1′′′	98.64
	2′′′	3.60	2′′′	53.44
	3′′′	4.26	3′′′	71.04
	4′′′	3.84	4′′′	70.38
	5′′′	4.35	5′′′	73.37
	$6'''_{a,b}$	3.45, 3.40	6′′′	43.39

$$R_{1p} = R_{1obs} - R_{1f} = \frac{p_b}{R_{1M}^{-1} + \tau_M} \quad (1)$$

where: R_{1obs} and R_{1f} are the spin-lattice relaxation rates measured in the presence and in the absence of the metal respectively, τ_M is the exchange lifetime from the bound to the free state, p_b is the molar fraction of the bound ligand, and R_{1M} is the spin-lattice relaxation rate of the copper-bound ligand. R_{1M} is accounted for by the following simplified equation [Equation (2)] reporting the dipole-dipole interaction, as provided by the Solomon–Bloembergen–Morgan theory.[18]

$$R_{1M} = \frac{1}{10}\left(\frac{\mu_0}{4\pi}\right)^2 \frac{\hbar^2\gamma_I^2\gamma_S^2}{r^6}\left\{\frac{\tau_c}{1+(\omega_I-\omega_S)^2\tau_c^2} + \frac{3\tau_c}{1+\omega_I^2\tau_c^2} + \frac{6\tau_c}{1+(\omega_I+\omega_S)^2\tau_c^2}\right\} \quad (2)$$

where: μ_0 is the vacuum permeability, γ_I and γ_S are the nuclear and electron magnetogyric ratios, ω_I and ω_S are the proton and electron Larmor frequencies, respectively, r is the proton–Cu^{II} distance and τ_c is the effective correlation time.

The proton spin-lattice relaxation rates were selectively affected, as also reported in Table 4, while no sizeable

change in chemical shift was detected. The relatively larger R_{1p} values experienced by the 2_{ax}, 2_{eq}, 5 and 1′ protons suggest that rings A and B of neomycin B are directly involved in the coordination of the Cu^{II} ion. ^{13}C paramagnetic relaxation rates, together with potentiometric data (Table 1 and Table 5), moreover suggest the 1 and 3 deprotonated amino groups (ring B) and 4′ deprotonated hydroxyl group (ring A) as the possible donor set.

Table 4. Paramagnetic contributions to proton longitudinal relaxation rates (R_{1p}, s^{-1}) of neomycin B, 9.9 mM in D_2O at pH 6.8 (value uncorrected for the isotopic effect), T = 298 K. Contributions were calculated as the difference between the R_1 values in the presence (R_{1obs}) and in the absence (R_{1f}) of $Cu(NO_3)_2$ [ratio Cu^{II}-neomycin: 1:100] and converted into copper-proton distances r_{Cu-H} through Equations (1) and (2) using $\tau_C = 2.73 \times 10^{-10}$ s and $\tau_M = 6.00 \times 10^{-4}$ s. Missing values are due to overlap among protons of the same ring.

Proton	R_{1f}	R_{1obs}	R_{1p}	R_{1M}	r_{Cu-H} [nm]
1, 3, 4, 6	–	–	–	–	–
2_{ax}	2.297	3.569	1.272	–18962	very near
2_{eq}	2.456	3.532	1.076	21564	0.276
5	1.337	2.276	0.939	7101	0.332
1′	1.165	2.336	1.171	–186079	very near
2′–6′	–	–	–	–	–
1″	0.976	1.596	0.620	2017	0.412
2″	0.826	1.207	0.381	835	0.475
3″	1.104	1.510	0.406	922	0.468
4″	0.865	1.432	0.567	1665	0.425
5″a	1.842	2.787	0.945	9019	0.330
5″b	1.974	2.772	0.798	4069	0.370
1‴	1.146	1.768	0.622	2032	0.412
2‴	0.818	1.799	0.981	11836	0.318
3‴	0.772	1.874	1.102	145752	0.259
4‴	1.058	1.687	0.629	2084	0.410
5‴	1.194	1.817	0.623	2039	0.328
6‴ab	1.771	2.721	0.95	9341	0.317

The correlation time in Equation (2) is generally determined by rotation of the metal complex. The reorientational dynamics of the complex was approximated by evaluating the motional correlation time of the free antibiotic in a water solution. This was accomplished by measuring the value of the cross-relaxation rate, σ, of the 2_{ax} and $2_{equiv.}$ protons of the ring B by means of Equation (3).[19]

$$\sigma = R^{bsel} - R^{sel} = \frac{1}{10}\left(\frac{\mu_0}{4\pi}\right)^2 \frac{\gamma_H^4 \hbar^2}{r^6}\left(\frac{6\tau_c}{1+4\omega_H^2\tau_c^2} - \tau_c\right) \quad (3)$$

where: r is the distance between vicinal protons (0.177 nm), and R^{bsel} and R^{sel} are the double- and single-selective spin-lattice relaxation rates, respectively. The value obtained was $\tau_c = 0.27 \pm 0.05$ ns at 298 K.

As stated in Equation (1), exchange of the ligand between free and bound states must be considered. In fact

Table 5. Paramagnetic contributions to carbon longitudinal relaxation rates (R_{1p}, s^{-1}) of neomycin B 9.9 mM in D_2O at pH 6.8 (value uncorrected for the isotopic effect), T = 298 K. Contributions were calculated as the difference between the R_1 values in the presence (R_{1obs}) and in the absence (R_{1f}) of $Cu(NO_3)_2$ [ratio Cu^{II}-neomycin B: 1:100] and converted into copper-carbon distances r_{C-Cu} [nm].

Carbon	R_{1f}	R_{1obs}	R_{1p}	r_{C-Cu} [nm]
1	2.196	3.812	1.616	0.337
2	2.669	2.900	0.231	0.465
3	3.417	6.716	3.299	0.293
4	2.463	3.223	0.760	0.384
5	2.611	3.401	0.790	0.382
6	2.313	2.477	0.164	0.491
1′	2.402	4.014	1.612	0.337
2′	3.004	4.954	1.950	0.325
3′	2.562	3.222	0.640	0.393
4′	2.487	3.401	0.914	0.372
5′	2.687	2.959	0.272	0.454
6′	3.994	4.009	0.015	0.603
1″	2.285	2.703	0.418	0.425
2″	2.462	3.206	0.744	0.386
3″	2.702	2.724	0.022	0.615
4″	2.569	3.175	0.606	0.399
5″	4.887	4.147	–0.740	–
1‴	2.976	4.022	1.046	0.363
2‴	2.405	3.262	0.857	0.377
3‴	2.287	3.160	0.873	0.375
4‴	2.451	3.406	0.955	0.370
5‴	2.163	3.175	1.012	0.366
6‴	3.702	4.156	0.454	0.417

R_{1M}, the structure-sensitive parameter, can be directly obtained from Equation (2) only in cases where fast exchange conditions ($R^{-1}_{1M} >> \tau_M$) prevail. The unusually small, although diverse, R_{1p} values suggest, by themselves, occurrence of a slow-intermediate exchange region, where R^{-1}_{1M} is equal or slightly smaller than τ_M. This being the case, both R^{-1}_{1M} and τ_M would contribute to R_{1p}. The contribution of exchange was measured by the temperature dependence of R_{1p}, which is well known in the literature.[20]

The temperature dependencies of the R_{1p} values of some protons are shown in Figure 3. The plots suggest that slow exchange conditions prevail (this justifies the relatively small paramagnetic effects), but that R_{1p} is close to its maximum where intermediate exchange conditions dominate. The exchange rates were calculated by fitting the initial part of the temperature dependent R_{1p} data (where $R_{1p} \approx p_b k_{off} = p_b/\tau_M$, τ_M being the exchange lifetime) with the Eyring equation [Equation (4)].[20]

$$\tau_M^{-1} = \frac{kT}{h} e^{-\frac{\Delta G^\#}{RT}}$$

$$\ln[R_{1p}] = \ln\left[p_b \frac{kT}{h}\right] - \frac{\Delta G^\#}{RT} \quad (4)$$

where: $\Delta G^\#$ is the free energy of activation for the dissociation process and p_b is approximated to the [Cu^{II}]/[neomycin B] ratio. An average value of $\tau_M = 0.60 \pm 0.03$ ms could be calculated.

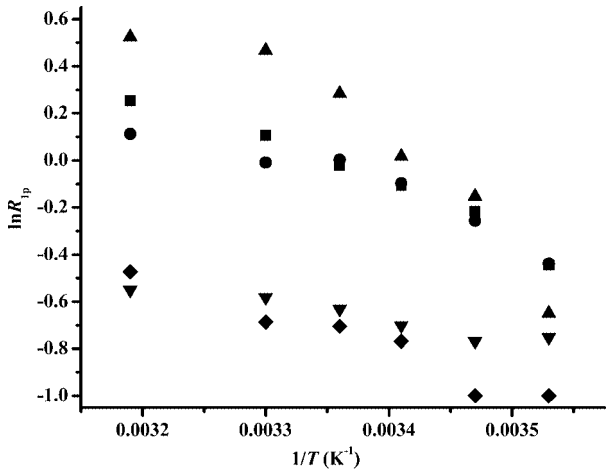

Figure 3. Temperature dependencies of paramagnetic relaxation rates (R_{1p}) of selected protons of neomycin B (9.9 mM) in D_2O (pH 6.8), in the presence of Cu^{II} ions at a concentration of 0.099 mM: 2_{ax} of ring B (■); 2_{eq} of ring B (●); 1′ of ring A (▲); 1″ of ring C (▼); 1‴ of ring D (♦).

Introducing the exchange time value into Equation (1) allowed us to extract all R_{1M} values from the R_{1p} ones. Since Equation (2) provides R_{1M} as a function of τ_c/r^6, taking the value of τ_c for the free ligand to be 0.27 ± 0.05 ns at 298 K, allowed us to calculate all copper–proton and copper–carbon distances, also shown in Table 4 and Table 5. The approximation used is not expected to introduce large errors in the calculated distances because the r^6 dependence minimizes even large errors (up to 50%) in the motional correlation time. The distances were then used as restraints in order to calculate the structure of the Cu^{II}-neomycin B complex in aqueous solution at pH 6.8. The suggested structure was supported by molecular mechanics and dynamics: an energy-minimized molecular model of Cu^{II}-neomycin B complex (Figure 4) was obtained by using the HYPERCHEM graphics package. The stick model of the complex shows the Cu^{II} ion bound to the two deprotonated amino groups of ring B, the 4′ deprotonated hydroxyl group of ring A and a water molecule added to reach the minimum set of donors. The 3‴-OH (ring D) and the 3-NH_2 (ring B) were found at a typical hydrogen bonding distance, such that further stabilization of the complex may be hypothesized. The obtained structure suggests that neomycin B wraps around Cu^{II} in a way that leaves the metal ion exposed to the water medium.

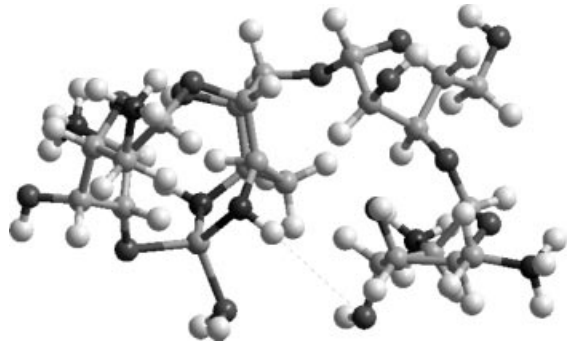

Figure 4. Structural model of the Cu^{II}-neomycin B 1:1 complex in water solution. The dashed line represents the hydrogen bond.

The above coordination model of CuH_2L is also supported by other spectroscopic methods (Table 6). The values of the A_{II} and g_{II} parameters calculated from the EPR spectra confirm the number of nitrogen donors around the metal ion. Moreover, the parameters of charge-transfer bands (CD, UV/Vis) and d-d bands (UV/Vis) change significantly with an increase in the concentration of this species (see Figure 2). The formation of two positive and one negative Cotton effects in the CD spectra (Figure 2, part a, Table 6) is observed. The effects at 260 and 300 nm most probably correspond to $NH_2 \rightarrow Cu^{II}$ CT transitions and those at 370 nm to the $O^- \rightarrow Cu^{II}$ one. The distinct shoulder on electronic absorption spectra around 355 nm suddenly appears around pH 5.5 and its intensity also increases with the rise of the CuH_2L fraction (Figure 2, part b). The d-d band parameters obtained from UV/Vis spectra reflect these changes, while the intensity of this band in the CD spectra is very low and remains at this level until about pH 10 (Figure 2, part b). It is worth stressing that all applied spectroscopic methods show persistence of spectral parameters with the appearance of the following three species. With an increase of pH to 9 solutions containing CuHL, CuL and $CuH_{-1}L$ complexes give very similar spectra. All these species differ from each other by the proton contents only. The values of their deprotonations fit the range 7–9, characteristic for amine group deprotonation.

Table 6. Spectroscopic parameters of particular complex forms of Cu^{II}-neomycin B, 1:1 system.

Species	UV/Vis[a]		CD[a]		EPR[b]	
	λ	ε	λ	$\Delta\varepsilon$	$A_{\parallel}$	$g_{\parallel}$
			700[c]	–0.23		
CuH_2L + CuHL +	616	65	370[d]	+0.54	184	2.24
CuL + $CuH_{-1}L$	356[sh]	270	300[e]	+1.77		
			261[e]	–5.51		

[a] λ [nm], ε and $\Delta\varepsilon$ [M^{-1} cm^{-1}]. [b] A_{II} [Gs]. [c] d-d transition band. [d] CT: $O^- \rightarrow Cu^{II}$. [e] CT: $NH_2 \rightarrow Cu^{II}$, [sh] shoulder.

At about pH 10, the solution of the Cu^{II}-neomycin complex changes its color from deep blue to violet. CD spectra obtained under these conditions present a total disappearance of the charge-transfer band at 370 nm and a distinct decrease of the band intensity at around 260 nm, probably suggesting the stepwise hydrolysis of the bound neomycin molecule, as already reported.[13] Mass spectra recognize this process already at pH 8.0, though to a very low extent (Table 2).

Two-Centered Cu^{II}-Neomycin B Complexes

A unique feature of the copper(II)-neomycin system is the formation of two-centered complexes, occurring at excess concentrations of the metal ion. Such complexes appear below pH 6, although in the pH range 4–6 mononuclear species also occur (Figure 5). However, their concentration

does not exceed 15% of the total amount of Cu^{II}. It is worth noting that species having the stoichiometry CuH_5L and CuH_4L, present in this system, do not appear in potentiometric titrations for the equimolar Cu^{II}-antibiotic system. It therefore seems likely that either the double excess of Cu^{II} ions over neomycin favors its deprotonation, and subsequent coordination to the metal, or the concentration of both complexes in the 1:1 system is too low for pH-metric detection. Table 7 shows the stability constants for dinuclear species, while Figure 5 presents the course of CD spectral parameters depending on the pH of the solution. The $\Delta\varepsilon$ values of d-d transition bands both for 1:1 and 2:1 systems are overlaid on the speciation diagram for the dinuclear Cu^{II}-neomycin complexes. Apparently, with an excess of the metal ion, an increase of the d-d band intensity follows the formation of the two-centered complexes. Around pH 7.5, where only the 2:1 complexes exist in solution, the CD parameters are stable (Figure 5).

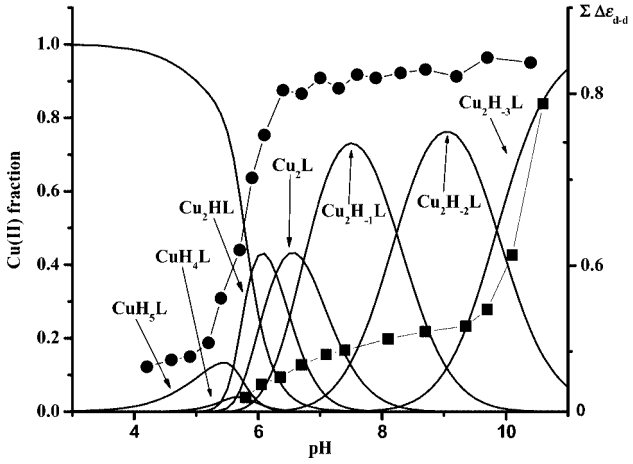

Figure 5. The speciation diagram for Cu^{II}-neomycin B complex at 2:1 molar ratio with $\Delta\varepsilon$ of d-d bands on CD spectra obtained for the 1:1 (■) and 2:1 (●) systems overlaid.

Table 7. The stability constants calculated for the system containing Cu^{II} ions and neomycin B at the molar ratio 2:1.

CuH_5L	43.73(3)
CuH_4L	37.64(6)
Cu_2HL	23.90(3)
Cu_2L	17.62(2)
$Cu_2H_{-1}L$	10.89(1)
$Cu_2H_{-2}L$	2.65(6)
$Cu_2H_{-3}L$	–7.19(2)

In order to ascertain the possibility of a Cu–Cu interaction, XAS spectra were obtained. Figure 6 shows the edge region of the spectra of the studied samples indicating different copper environments while keeping the edge energy values characteristic of Cu^{II} constant, as judged by the position of the main transition at about 8990 eV. The edge shape is characteristic for Cu^{II} complexed to nitrogen or oxygen donors.[21] The 1s-3d pre-edge absorption at ca. 8980 eV are all extremely small and indicate centrosymmetric Cu^{II} binding sites as present in Jahn–Teller distorted tetragonal or square-planar copper complexes.[22] Hence we conclude that the concentrated samples (1 and 2), regardless of the molar ratio, show similar edges resembling that of the free Cu^{II}_{aq}, while the 2 mM sample (3) displays 1s-4p transitions at about 8988 eV and more complex white line transitions (see Figure 6).

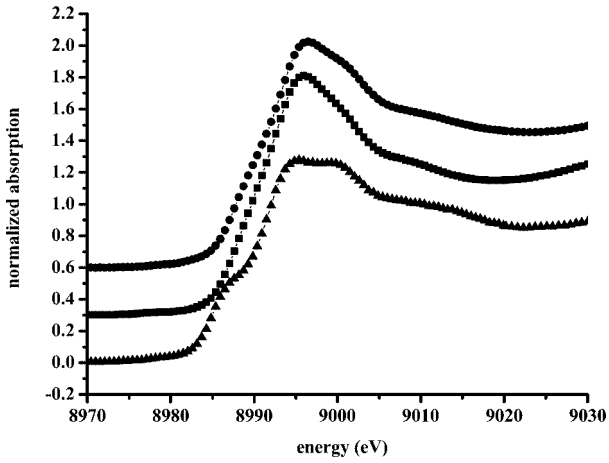

Figure 6. Comparison of the X-ray absorption edges for the Cu^{II}-neomycin B 2:1 complex, Cu^{II} 100 mM (■), Cu^{II}-neomycin B 2:1 complex, Cu^{II} 2 mM (▲) and Cu^{II}-neomycin B 1:1 complex, Cu^{II} 100 mM (●).

The EXAFS spectrum of the Cu^{II}-neomycin B complex 2:1, (100 mM, sample 1) together with its Fourier transform is reported in Figure 7, parts a,b. The spectrum is characteristic of all light O/N type scatterers and, despite the presence of slight distortions due to multiple scattering effects from outer shell atoms, it can be well simulated without introducing multiple scattering contributions into the calculations. The contribution to the total EXAFS of the first shell ligand can be evaluated in four O/N divided into two shells of two donors at 1.94(1) Å and two donors at 2.02(1) Å (see Table 8). Adding a further shell of two N/O atoms at 2.74(2) Å significantly improves the fit leading to a classical Jahn–Teller distorted elongated octahedron for the Cu^{II} coordination. As already indicated by the edge shape the EXAFS spectrum of sample 2 (Cu^{II}-neomycin B 1:1 complex, 100 mM) as with the previous one, can be simulated by a 4+2 type of Cu^{II} coordination consisting of four N/O atoms at 1.98(1) Å and two N/O atoms at 2.32 Å and 2.83 Å, respectively.

Due to the low copper concentration the spectrum of sample 3 (Cu^{II}-neomycin B 2:1 complex, 2 mM) is much noisier than the others. However, the EXAFS (Figure 8, a) displays features, which can be reproduced only by introducing multiple scattering (MS) path contributions from atoms lying in a rigid scaffold containing almost colinear arrangements of atoms. Together with the shape of the edge region, this evidences a significantly different Cu^{II} coordination with respect to the same complex in a more concentrated solution (sample 2). Here Cu^{II} is bound to two N/O atoms at 1.96(1) and 2.00(1) Å and two N/O atoms at 1.91(1) and 1.96(1) Å. The outer shell features evident in the spectrum Fourier transform (Figure 8, b) can be adequately modeled by the MS from outer shell atoms bound

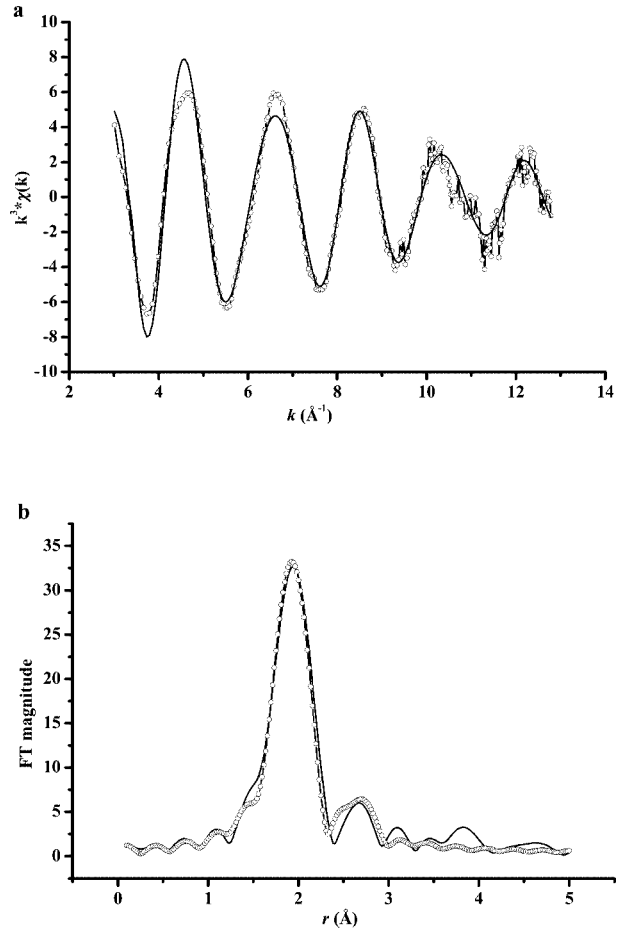

Figure 7. Comparison of experimental (open circles) and theoretical (continuous line) EXAFS data (a) and of their Fourier transform (b) for the Cu^{II}-neomycin B 2:1 complex at 100 mM concentration.

Table 8. Results of data analysis of the full EXAFS spectra for the Cu^{II}-neomycin B, 1:1 and 2:1 systems.

Sample	Shell	Distance [Å]	DWF[a] $2\sigma^2$ [Å^2]	R_{exafs}[b] (%)	FI[b]
1	2N/O	1.93(1)	0.004(1)	24.5	0.39
	2N/O	2.01(1)	0.004(1)		
	2N/O	2.74(2)	0.016(2)		
2	4N/O	1.98(1)	0.008(2)	27.0	0.42
	1N/O	2.32(1)	0.003(2)		
	1N/O	2.83(2)	0.008(3)		
3 (MS)	1N/O	1.96(1)	0.004(2)	42.1	0.69
	1N/O	2.00(1)	0.005(1)		
	1N/O	1.91(1)	0.002(1)		
	1N/O	1.96(1)	0.002(2)		
	1C	2.78(2)	0.009(2)		
	1C	2.75(2)	0.002(2)		
	1N	4.04(2)	0.009(3)		
	1O	3.98(1)	0.014(4)		

[a] DWF is the Debye–Waller factor. [b] R_{exafs} and the fit index (FI) are indicators of the fit quality as reported in the Experimental Section.

to a rigid, bidentate, N/O type ligand. The presence of MS effects makes it impossible to detect the probable presence of two axial O/N ligands between 2.3–2.8 Å as seen in samples 1–2.

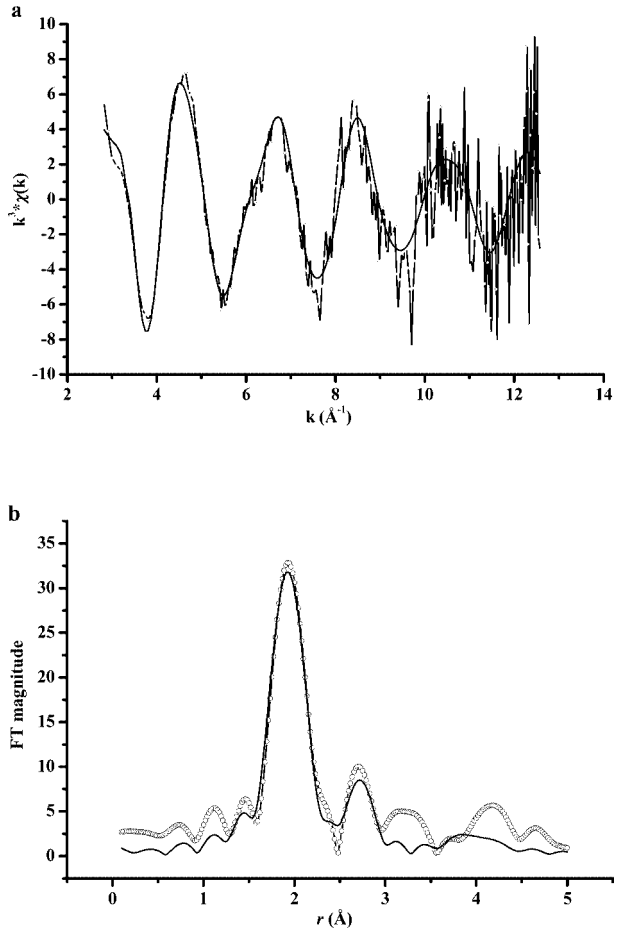

Figure 8. Comparison of experimental (open circles) and theoretical (continuous line) EXAFS data (a) and of their Fourier transform (b) for the Cu^{II}-neomycin B 2:1 complex at 2 mM concentration. The fitting parameters are reported in Table 8.

EXAFS is able to detect metal-metal distances when they are in the 3.5–4.0 Å range. Furthermore, at longer distances the Cu–Cu scattering in nonordered systems like solutions is very weak and can be hidden in the background due to the scattering of light atoms (C, N, O), lying at about the same distance from the metal.[23] However, there is no evidence of Cu–Cu scattering in the case of the neomycin complexes. If there are two Cu atoms bound per neomycin molecule, they should be located at distances larger than 3.5 Å. Lack of the spin relaxation on the EPR spectra, which were obtained under the same conditions, confirms that both metal ions are separated and are most probably located at different rings of the antibiotic.

Mass spectrometry brings additional evidence for the Cu^{II}_2-neomycin complex formation. The distinct peak at *m*/*z* of ca. 739 is observed (Table 2). Its intensity is intermediate but several further peaks originating from the variety of adducts occur at higher values of *m*/*z*. The peaks with

m/*z* ca. 788, 820, 840, 857 and 918 correspond with adducts formed by two Na, two K, perchlorate, Na + sulfate and three carbonate ions, respectively (data not shown in Table 2).

Conclusions

The results obtained indicate that neomycin B, compared with the other previously investigated aminoglycosides, binds copper(II) ions with the highest affinity. The reason that it happens may be found within the binding pattern. Three-ring aminoglycosides, i.e. kanamycin A and B, tobramycin or geneticin, coordinate Cu^{II} ion mostly by their terminal amino sugar donors and not by the amines of the deoxystreptamine residue, in contrast with what has been presently demonstrated in the case of the four-ring neomycin. Cu^{II} coordination by the donors of this ring not only leads to an increase in stability of the complexes but also leaves the amino groups of the A and D rings uninvolved in any interaction with the metal ion. As a consequence, at excess copper(II) concentrations, a second metal ion may be bound by neomycin B, most probably at a site provided by ring D. In fact, none of its donor groups is directly involved in the coordination process of the first Cu^{II}, while ring A donates a hydroxyl group for axial complex stabilization. Formation of dinuclear species is a unique feature of neomycin B within all of the Cu^{II}-aminoglycoside systems investigated so far.

Experimental Section

Materials: Neomycin B, $CuCl_2$, $Cu(ClO_4)_2$, $Cu(NO_3)_2$, KNO_3, $NaClO_4$, 1,2-ethanediol, DCl, NaOD, TSP-d_4, 3-(trimethylsilyl)-[2,2,3,3-d_4] propionate sodium salt and all other simple chemicals were purchased from Sigma Chemical Co. (St. Louis, MO). Deuterium oxide (99.95%) was obtained from Spectra2000 s.r.l.

Potentiometry: Potentiometric titrations of neomycin B and its complexes with Cu^{II} in the presence of 0.1 M KNO_3 were performed at 25 °C using pH-metric titrations over the pH range 3–12 (Molspin automatic titrator, Molspin Ltd, Newcastle upon Tyne, UK) with 0.1 M NaOH as titrant. Changes in pH were monitored with a combined glass-Ag/AgCl electrode (ATI Russell pH Ltd, Fife, Scotland) calibrated daily in hydrogen ion concentrations by HNO_3 titrations.[24] Samples contained 1 mM neomycin B and Cu^{II}: antibiotic molar ratios of 1:1, 1:2 and 2:1 were used. The data were analyzed using the SUPERQUAD program.[25] Standard deviations computed by the SUPERQUAD program refer to random errors only.

Electronic Absorption (UV/Vis): The electronic absorption spectra were recorded at 25 °C with a Beckman DU-650 (Beckman, Palo Alto, CA) spectrophotometer over the spectral range of 200–900 nm, in a 1 cm cell. The samples contained a 2.5 mM Cu^{II}-neomycin B complex at a 1:1 molar ratio. The experiments were performed in 0.1 M $NaClO_4$ to keep a constant ionic strength, analogous to that used in the potentiometric titrations.

CD Spectroscopy: The spectra were recorded at 25 °C with a Jasco J-715 spectropolarimeter (JASCO, Japan Spectroscopic Co., Hiroshima, Japan), over the range of 200–800 nm, using a 0.5-cm cell. Samples contained a 1:1 or 2:1 Cu^{II}-to-neomycin B ratio at complex concentration of 2.5 mM. For the electronic absorption spectroscopic measurements a 0.1 M aqueous $NaClO_4$ solution was used. The spectra are expressed in terms of $\Delta\varepsilon = \varepsilon_l - \varepsilon_r$, where ε_l and ε_r are molar absorption coefficients for left and right circularly polarized light, respectively.

EPR Spectroscopy: The spectra of the Cu^{II} complex with neomycin B were recorded at 77 K with a Bruker ESP 300E spectrometer (Karlsruhe, Germany) at the X-band frequency (9.3 GHz). 1,2-ethanediol: water (1:2) was used as solvent in the low-temperature experiments to obtain homogeneity of the frozen samples. The concentrations of Cu^{II} in the samples were of 5 mM and Cu^{II}-to-neomycin B molar ratios were 1:1 and 2:1.

NMR Spectroscopy: Neomycin B solutions were made in deuterium oxide (99.95%), adjusted to a 0.1 M ionic strength with KNO_3 and carefully deoxygenated through a freezing-vacuum pumping-sealing-thawing procedure. The desired concentration of copper ions was achieved by using a stock solution of copper nitrate in deuterium oxide (molar ratio Cu^{II}-neomycin: 1:100). The pH was adjusted with either DCl or NaOD. NMR spectroscopic experiments were carried out at 14.1 T and at a controlled temperature (±0.1 K) with a Bruker Avance 600 spectrometer equipped with a Silicon Graphics workstation. TSP-d_4 was used as the internal reference standard. The proton resonance assignment was obtained by COSY and ROESY experiments. Rotating frame Overhauser enhancement spectroscopy (ROESY) was performed at a mixing time of 300 ms and the radio-frequency strength for the spin-lock field was 1.9 KHz. 2D ^1H ^{13}C HSQC shift correlation spectra were obtained in order to detect and assign ^{13}C NMR spectra at relatively low concentrations. Proton spin-lattice relaxation rates ($R_1 = 1/T_1$) were measured with the inversion recovery pulse sequence or with a combination of it with 2D TOCSY, when imposed by resolution limits. This was obtained by introducing a ^1H 180° pulse followed by a variable delay in front of the TOCSY sequence. Relaxation rates were calculated with regression analysis of the initial recovery curves of longitudinal magnetization components, leading to errors in the range of ±3%. A DANTE pulse train was used to measure selective proton spin-lattice relaxation rates.[26]

Molecular Mechanics and Dynamics Calculations: Molecular structures were generated by the HYPERCHEM software package [HYPERCHEM, Hypercube release 7.5 for Windows; Hypercube Inc.: Waterloo, ON, 2002], implemented on a Pentium 120 MHz PC. Charges were calculated by ZINDO-1 semi-empirical methods, and the model was then subjected to 25 ps unrestrained molecular dynamics at 300 K with the MM+ force field. The H–Cu and C–Cu distances, as obtained by NMR spectroscopic experiments, were introduced as restraints for the final 25 ps MD run at 300 K.

XAS Data Collection and Analysis: XAS data at the copper edge were collected at DESY (Hamburg, Germany) with the EMBL bending magnet beam line D2 equipped with a Si(111) double crystal monochromator with an energy resolution of 1.6 eV at 8980 eV. The DORIS-III storage ring was operated under normal conditions (4.5 GeV, 90–140 mA). The second monochromator crystal was detuned to 50% of its peak intensity in order to reject higher harmonics. Ionization chambers in front of and behind the sample were used to monitor the beam intensity. The sample cells were mounted in a 2-stage Displex cryostat (modified Oxford instruments) and kept at 20 K during data collection.

The samples used for data collection are as follows:

1. Cu^{II}-neomycin B complex at a 2:1 molar ratio, Cu^{II} conc. 100 mM

2. Cu^{II}-neomycin B complex at a 1:1 molar ratio, Cu^{II} conc. 100 mM

3. Cu^{II}-neomycin B complex at a 2:1 molar ratio, Cu^{II} conc. 2 mM

For samples 1 and 2 the data were collected at the copper edge (ca. 8990.0 eV at the edge jump inflection point) by monitoring the sample absorption, while for the more dilute sample 3 the Cu-K_α fluorescence was detected with an energy discriminating 13 element Ge solid state detector (Canberra). The Bragg reflections of a static Si(220) crystal in back-reflection geometry have been used for the absolute energy calibration of the copper spectra.[22] For samples 1 and 2 three to eight spectra were collected for each sample from 8410 to 9810 eV with variable step widths. In the XANES and EXAFS regions steps of 0.3 and 0.6–1.5 eV were used, respectively. For sample 3 only two scans could be collected and the final spectrum resulted from the averaging. The scans spanned the 8500–9810 eV energy range with variable steps in the different regions of the spectrum. After inspection of each scan for edge consistency, the data were normalized by the edge jump and averaged. The EXAFS was then extracted by subtracting the slowly varying atomic background fitted with a cubic spline. Data reduction to extract the EXAFS spectrum was based on standard procedures and performed with the EXPROG software package.[27] The full, k^3 weighted, EXAFS spectra have been compared with theoretical simulations obtained by utilizing the rapid curved multiple scattering theory implemented in the set of programs EXCURVE 9.20.[28] The whole spectrum was analyzed by simulation by varying the atom types and the coordination numbers and iteratively refining the distance (R) and the Debye–Waller factor ($2\sigma^2$) for each atomic shell. The quality of the fit was assessed by the goodness of fit function through the parameter ε^2 which accounts for the degree of over determinacy[29] and by the R factor as defined within EXCURVE 9.20.[28] The pre-edge peak (1s-3d electronic transition at ca. 8980 eV) areas were calculated by subtracting an arctangent function from the normalized edge spectra and integrating over the range 8975–8985 eV.

Mass Spectrometry: The mass spectra were obtained with a Finnigan Mat TSQ 700 instrument (Thermo-Finnigan, Bremen, Germany), using the ESI (electro-spray ionization) technique with N_2 as carrier gas, and flow-rate of 2 μL/min. Three kinds of samples were investigated at pH 8.0 (adjusted with acetic acid and ammonium carbonate): free neomycin B and Cu^{II}-neomycin B complex at 1:1 and 2:1 ratios. All samples were prepared as water solutions. Then methanol was added to a final concentration of 50%, in order to decrease surface tension during sample evaporation. Final sample concentrations were: neomycin B, 0.25 mM and Cu^{II}, 0.25 or 0.5 mM.

Acknowledgments

The authors wish to thank Dr. Wolfram Meyer-Klaucke from EMBL Outstation in Hamburg for collecting XAS data. W. Szczepanik thanks the Foundation for Polish Science (FNP) for the Annual Stipend for Young Scientists. This work was supported by the Polish State Committee for Scientific Research (KBN), grant no. 4 T09A 179 25, for the period 2003–2006.

[1] W. G. Barnes, *Aminoglycoside Antibiotics: A Guide to Therapy*, CRC Press, Inc., Boca Raton, Florida, **1984**.
[2] W. Szczepanik, J. Ciesiołka, J. Wrzesiński, J. Skała, M. Jeżowska-Bojczuk, *Dalton Trans.* **2003**, 1488–1494.
[3] M. Jeżowska-Bojczuk, A. Karaczyn, W. Bal, *J. Inorg. Biochem.* **1998**, *71*, 129–134.
[4] W. Szczepanik, P. Kaczmarek, J. Sobczak, W. Bal, K. Gatner, M. Jeżowska-Bojczuk, *New J. Chem.* **2002**, *26*, 1507–1514.
[5] M. Jeżowska-Bojczuk, W. Bal, H. Kozłowski, *Inorg. Chim. Acta* **1998**, *275–276*, 541–545.
[6] M. Jeżowska-Bojczuk, A. Karaczyn, H. Kozłowski, *Carbohydr. Res.* **1998**, *313*, 265–269.
[7] W. Szczepanik, E. Dworniczek, J. Ciesiołka, J. Wrzesiński, J. Skała, M. Jeżowska-Bojczuk, *J. Inorg. Biochem.* **2003**, *94*, 355–364.
[8] M. C. Linder, *Copper Metabolism*, Plenum Press, New York, **1991**.
[9] N. E. Moat, T. E. Evans, G. J. Quinlan, J. M. Gutteridge, *FEBS Lett.* **1993**, *328*, 103–106.
[10] M. C. Linder, M. Hazegh-Azam, *Am. J. Clin. Nutr.* **1996**, *63*, 797–811.
[11] K. Aihara, Y. Nishi, S. Hatano, M. Kihara, K. Yoshimitsu, N. Takeichi, T. Ito, H. Ezaki, T. Usui, *Am. J. Clin. Nutr.* **1984**, *40*, 26–35.
[12] S. M. Abu-El-Wafa, M. A. El-Ries, F. M. Abou-Attia, R. M. Issa, *Anal. Lett.* **1989**, *22*, 2703–2716.
[13] A. Sreedhara, J. D. Freed, J. A. Cowan, *J. Am. Chem. Soc.* **2000**, *122*, 8814–8824.
[14] R. E. Botto, B. Coxon, *J. Am. Chem. Soc.* **1983**, *105*, 1021–1028.
[15] B. Noszal, in *Biocoordination C: Coordination Equilibria in Biological Active Systems* (Ed.: K. Burger), Ellis Harwood Ltd, London, **1990**.
[16] D. G. Reid, K. Gajjar, *J. Biol. Chem.* **1987**, *262*, 7967–7972.
[17] R. E. Botto, B. Coxon, *J. Carbohydr. Chem.* **1984**, *3*, 545–563.
[18] I. Solomon, *Phys. Rev.* **1955**, *99*, 559–565.
[19] L. D. Hall, H. D. W. Hill, *J. Am. Chem. Soc.* **1976**, *98*, 1269–1270.
[20] I. Bertini, C. Luchinat, *NMR of Paramagnetic Substances*, *Coord. Chem. Rev.* 150, ed.1, Elsevier, Amsterdam, **1996**, pp. 1–300.
[21] R. F. Pettifer, C. Hermes, *J. Appl. Crystallogr.* **1985**, *18*, 404–412.
[22] L. S. Kau, D. J. Spira-Solomon, J. E. Penner-Hahn, K. O. Hodgson, E. I. Solomon, *J. Am. Chem. Soc.* **1987**, *109*, 6433–6442.
[23] P. J. Riggs-Gelasco, T. L. Stemmler, J. E. Penner-Hahn, *Coord. Chem. Rev.* **1995**, *144*, 245–286.
[24] H. Irving, M. G. Miles, L. D. Pettit, *Anal. Chim. Acta* **1967**, *38*, 475–488.
[25] P. Gans, A. Sabatini, A. Vacca, *J. Chem. Soc. Dalton Trans.* **1985**, 1195–1200.
[26] G. A. Morris, R. Freeman, *J. Magn. Reson.* **1978**, *29*, 433–462.
[27] H. F. Nolting, C. Hermes, EXPROG: EMBL EXAFS data analysis and evaluation program package for PC/AT. European Molecular Biology Laboratory, c/o DESY, Hamburg, **1993**.
[28] N. Binsted, S. S. Hasnain, *J. Synchrotron Radiat.* **1996**, *3*, 185–196.
[29] P. A. Lee, J. B. Pendry, *Phys. Rev. B* **1975**, *11*, 2795–2811.

Received: February 1, 2005
Published Online: July 4, 2005

